Available online at www.sciencedirect.com
SCIENCE DIRECT®
International Journal of Heat and Mass Transfer 47 (2004) 1289–1296
International Journal of HEAT and MASS TRANSFER
www.elsevier.com/locate/ijhmt

Effect of aspect ratio on forced convection heat transfer from cylinders

B.H. Chang [a,*], A.F. Mills [b]

[a] Department of Computer Aided Mechanical Design, Incheon City College, Incheon 406-131, South Korea
[b] Mechanical and Aerospace Engineering Department, University of California, Los Angeles, CA 90095, USA

Received 18 April 2003; received in revised form 1 September 2003

Abstract

The effect of aspect ratio on heat transfer to a cylinder in cross flow of air has been studied experimentally. The aspect ratios tested were AR = 12, 10.8, 8.5 and 6 for a Reynolds number range of $6300 < Re_D > 50,960$. The tunnel blockage ratio was 8.6%, and the cylinder had a uniform wall temperature. Local heat transfer coefficients were measured at various positions along the cylinders. Heat transfer rates at the centerplane on the rear of the cylinder increased with decreasing aspect ratio. At AR = 12 there was also a marked increase along the cylinder as the wall was approached: at AR = 6 the heat transfer was uniformly high along the cylinder. Consequently, circumferentially averaged and total averaged Nusselt numbers increased with decreasing aspect ratio. For example, on the centerline at $Re_D = 33,740$, $Nu_{180°}/Nu_{0°}$ was 44% higher for AR = 6 than for AR = 12, and circumferentially averaged values were 14% higher. Correlations for the averaged Nusselt numbers are presented that account for the effects of aspect ratio, tunnel blockage and free stream turbulence.

1. Introduction

Forced convection heat transfer from a cylinder in crossflow has been the subject of many studies. In excess of 100 papers have reported experimental data for local and average heat transfer. Of primary interest has been the dependence of Nusselt number on the Reynolds and Prandtl numbers, and the proper accounting for variable property effects. However, it is known that a number of secondary flow parameters influence experimental data, of which the most important are freestream turbulence, tunnel blockage and aspect ratio. Correlations that appear in standard heat transfer texts and handbooks usually ignore the effects of these parameters, that is, assume that they are negligible. The effects of freestream turbulence and tunnel blockage have been the subject of a number useful studies in which these parameters have been systematically varied. On the other hand, there appears to have been no studies in which aspect ratio has been systematically varied. Furthermore, there is evidence that there is interplay between these effects; particular between blockage and aspect ratio: as a result, the data available from the literature are sometimes of less utility than may be immediately apparent.

The focus of this paper is the effect of aspect ratio. A literature survey suggests that, as the aspect ratio (AR) decreases below about 12, heat transfer on the rear of the cylinder increases, and consequently the average Nusselt number increases. But the evidence is limited to a few Reynolds numbers and requires comparison of results obtained by different investigators, at different blockages, and at possibly different turbulence levels. Since all these three parameters cause an increase in heat transfer, it is difficult to make unambiguous comparisons. As a result the effect of aspect ratio is sometimes ignored even when it is a relevant parameter. The two comprehensive review articles on cylinder heat transfer, namely by Zukauskas [1] and Morgan [2] give much information concerning the effects of free stream turbulence and tunnel blockage, but essentially ignore the

* Corresponding author. Tel.: +82-327608693; fax.: +82-327608697.
E-mail addresses: bhchang@icc.ac.kr (B.H. Chang), amills@ucla.edu (A.F. Mills).

0017-9310/$ - see front matter © 2003 Elsevier Ltd. All rights reserved.
doi:10.1016/j.ijheatmasstransfer.2003.09.013

Nomenclature

AR	aspect ratio cylinder, L/D
D	diameter of cylinder
H	test section height
k	thermal conductivity
L	length of the cylinder
Nu	Nusselt number, hD/k
$\overline{Nu}_{\mathrm{D}}$	circumferentially averaged Nusselt number
Nu_{avg}	cylinder surface averaged Nusselt number
Nu_0	stagnation Nusselt number
U	freestream velocity
Pr	Prandtl number
Re_{D}	Reynolds number, UD/v

Greek symbol

v	kinematic viscosity

effect of aspect ratio. The correlation for average heat transfer of Churchill and Bernstein [3] is widely used. These authors state that their correlation is a lower bound, and free stream turbulence, end effects, and tunnel blockage may increase the heat transfer rate. Yet they include results of Schmidt and Wenner [4] taken with cylinders of aspect ratios of 1–12 in the data base used to develop the correlation.

In the present context, the geometry consists of a single cylinder spanning a duct: the aspect ratio is then the duct width divided by cylinder diameter, $\mathrm{AR} = L/D$. We are not considering a cylinder of finite length located in a large duct: in this case the effect of aspect ratio is due to heat transfer from the ends of the cylinder. Quarmby and Al-Fakhri [4] have reported a detailed study of this different problem. In our case, aspect ratio affects the flow and heat transfer through the three-dimensional separated flow that forms due to the interaction of the boundary layer on the duct wall with the cylinder. A horseshoe vortex system is the main feature of this flow, and has been studied using flow visualization methods by, for example, Hunt et al. [5]. There is in first instance a wall effect, that is, heat transfer rates vary along the cylinders as the wall is approached, and hence an effect of aspect ratio. However, there is also an effect of the duct constraining the wake behind the cylinder. The wall effect has been studied by Goldstein and Karni [6], but the effect of duct width has not been studied. The effect of duct width is particularly important because in most experimental studies of heat transfer from cylinders, measurements are made at the center of the duct to minimize errors due to heat loss through the ends of the test cylinder. Sometimes guard heaters are used [7] or simply the aspect ratio is considered to be large enough to ignore possible errors at the centerplane. The wall effect introduces yet another parameter into the problem, that is, the nature and thickness of the wall boundary layer. Thus Goldstein and Karni [6] used distance from the wall divided by boundary layer displacement thickness to characterize distance from the wall when presenting their data.

The purpose of our study was to show aspect ratio effects in an unambiguous manner. Given the large number of parameters it was infeasible to obtain a comprehensive database. Tests were performed over a Reynolds number range of 6300–50,000 and aspect ratios of 6–12. The tunnel blockage was constant at 8.6%, and freestream turbulence was low enough to ignore its effect. Local Nusselt number distributions were obtained at the center plane, and at distances of 1/8, 1/4 and 1/2 of the half-span of the duct, measured from the wall. The wall boundary layer upstream of the test cylinder was essentially the same for AR values of 6, 8.5 and 10.8, but was different for $\mathrm{AR} = 12$, for which the complete width of the wind tunnel was used.

1.1. Apparatus and test procedures

The test cylinder, shown in Fig. 1, is made from copper, has a 3.395 cm outside diameter, a 2.75 mm wall thickness, and is 20 cm long. It is heated by a 75 W, 12 Ω Inconel/Kapton foil heater heated on its inner surface. A RdF microfoil heat flux sensor is located on the centerplane of the cylinder, and is 6.35 mm wide and 15.9 mm long. The sensor also contains a type T thermocouple to measure the wall temperature. The manufacturer supplied calibration constant for the heat flux meter is 0.408 μV/(Btu/ft^2 h). The free stream temperature is measured by a type T thermocouple. Data acquisition is performed by a Strawberry Tree Connection Mini-16 system and the data is fed to a PC for processing and display. The suction type wind tunnel has a 40.6 cm wide, 39.4 cm high test section with a Howden–Buffalo fan driven

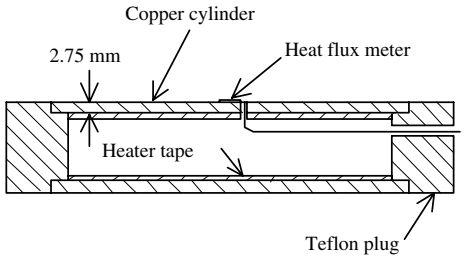

Fig. 1. Test cylinder.

through a Magnetek GPD 505 variable speed controller. The contraction area ratio between the intake chamber and the test section is 15, and the intake chamber had screens to produce a uniform velocity distribution. The length of the test section was 3.66 m and the length of the entire wind tunnel was 10.2 m. The air speed in the test section was measured using a pitot tube and inclined manometer. The 20 cm test cylinder is supported on insulated extensions to span the 40.6 cm wide test section. Aspect ratio is varied by inserting plates into the wind tunnel: the plates have sharp leading edges located 0.457 m upstream of the test cylinders. However, for AR = 12 the complete width of the tunnel was used, and the test cylinder was 1.66 m downstream of the contraction. The complete test cylinder assembly can be moved relative to the plates so that the one sensor can be used to obtain heat transfer data and any location from the effective duct wall.

For a test run, an aspect ratio, sensor location and tunnel speed were selected. Local heat transfer was obtained at 10° intervals by rotating the cylinder (2.5° intervals were used when the local Nusselt number variation warranted it). The wall to free stream temperature was maintained at approximately 10 K in order to have small and consistent effects of fluid property variation. Particular care was taken when obtaining data on the rear of the cylinder due to the inherently unsteady character of the flow and the resulting heat transfer. The local Nusselt number was calculated in real time by the PC: the displayed values were recorded at 2 s intervals over 50 s, and then averaged. The difference in the Nusselt number averaged over 25 s and that averaged over 75 s was within 1.5% over the entire cylinder. This approach assured that the heat flux and temperature difference used to compute the Nusselt number were in phase. The time averaged values were generally reproducible to within 1% over the front and 3% over the rear portion.

2. Results and discussion

Numerous studies have shown excellent agreement between measured stagnation line heat transfer rates with laminar boundary layer theory, provided free stream turbulence is below a critical value. One correlation of numerical solutions of the wedge flow equation often seen is [8]

$$Nu = 1.145 Re_D^{1/2} Pr^{0.4}, \quad 0.5 < Pr < 10 \tag{1}$$

Results reported by, for example, Achenbach [7], van Meel [9] and Kestin [10] show a reliable method of calibrating microfoil heat flux sensors is to use measured stagnation line heat transfer data in conjunction with Eq. (1) to give a sensor calibration constant. We and other workers e.g., Scholten and Murray [11], have found that the manufacturer supplied calibration constants for RdF sensors are unreliable: indeed, the company is unable to give a meaningful tolerance on the constant supplied. However, the calibration constant is not explicitly required. What is of interest are the ratios of local and average Nusselt numbers to the stagnation line value, because Eq. (1) will be the best estimate of stagnation line heat transfer in possible applications of our results. Scholten and Murray used a similar approach to report their results for gas-particle flows.

The results presented here are ratios of local or average Nusselt numbers to the stagnation line value. As a consequence any bias errors in the measurements of heat flux and temperature difference are irrelevant, and the only significant precision error is due to the unsteady nature of the heat transfer on the rear of the cylinder. Using the procedure described in the previous section we estimate an uncertainty in local Nusselt numbers less than 3%. The only significant source of error in our reported Reynolds numbers is due to bias error in the air speed measurement and is estimated not to exceed 2%. Since Reynolds number has only a weak effect on the local Nusselt number variation, this possible error is of no concern. As will be discussed later, the relevant "uncertainty" in our results is due to the effect of parameters such as blockage, free stream turbulence and the wall boundary layer thickness.

Fig. 2 shows the local Nusselt number around the cylinder at the center and at distances of 1/4, 1/6, 1/12 of the duct width from the wall for AR = 6. The heat transfer rates are generally higher as the wall is approached, but the profiles are very close to each other. The increases in the stagnation and the rear ($\theta = 180°$) Nusselt number at 1/12 L from the wall are only 3.8% and 3.4% higher than the centerline values respectively. The Nusselt number decreases to a minimum at around

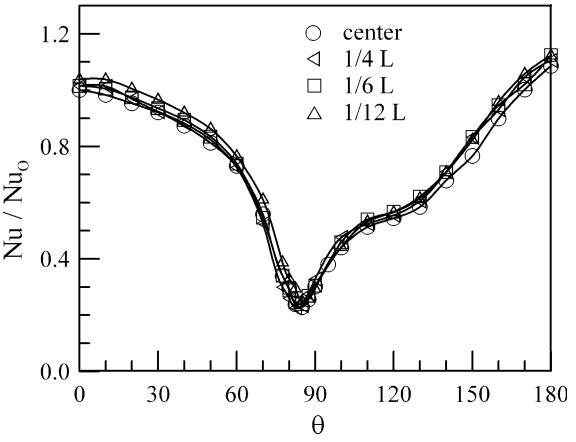

Fig. 2. Nusselt number profile for AR = 6, $Re = 33,740$.

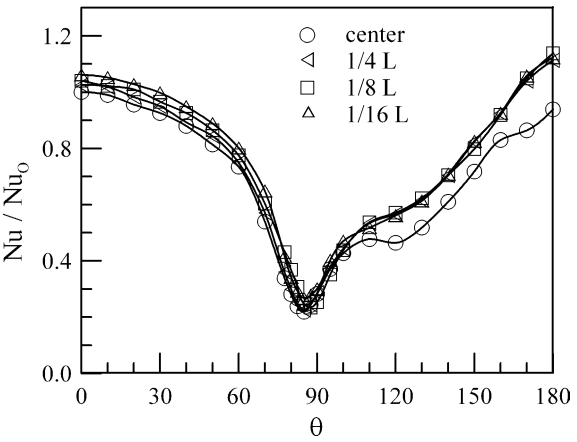

Fig. 3. Nusselt number profile for AR = 8.5, $Re = 33,740$.

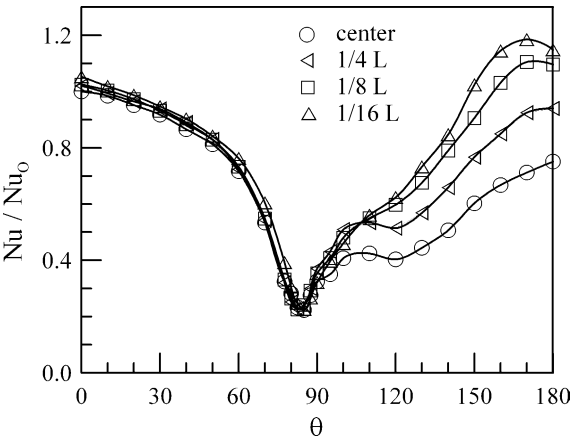

Fig. 5. Nusselt number profile for AR = 12, $Re = 33,740$.

85° near the separation point. The change of the slope in the distribution of Nusselt number after the separation point indicates an existence of a vortex, and the inflection point may correspond to the point of the maximum shear stress. Continued increase in Nusselt number after about 130° is due to a separate larger vortex, and reattachment of the flow behind the cylinder is expected at around 180°. However the vortices are unsteady and the resulting effects are time-averaged. The Nusselt number profiles for AR = 8.5 in Fig. 3 show that the centerline Nusselt number at $\theta = 180°$ is 16.4% lower than that at 1/16 L from the wall. The heat transfer rates at the rear of the cylinder between 1/4 and 1/16 L from the wall appear almost identical. A gradual change in heat transfer in the rear of the cylinder over the axial distance can be seen in the results for AR = 10.8 in Fig. 4. Large variations in Nusselt number along the cylinder can be seen in the results for AR = 12 in Fig. 5. The increase of the stagnation heat transfer at 1/16 L from the wall is only 5.3% over the centerline value, but the increase in *Nu* at $\theta = 180°$ is 53%. Similar trends were found for $Re = 50,960$. Goldstein and Karni's [6] results for AR = 12, blockage ratio of 4.2%, and $Re = 19,000$ also show a large increase at the back of the cylinder. Their results showed that at 1/12 L from the wall, the increase in Sherwood number at $\theta = 176$–178° is about 40% over the centerline value. In the present experiment, the wall boundary layer thickness upstream of the test cylinder for AR = 12 is estimated to be around 6.4 mm, and this is about twice the boundary layer thickness of 3.4 mm for AR = 6, 8.5 and 10.8. However, the ratio of the boundary layer thickness over the half width of the duct may be a more important parameter than the boundary layer thickness itself. Also, this ratio is very small (2–3.4%) for all the aspect ratios, and the nearest location of heat transfer measurement from the wall is 1/8 of the half width or 12.5%. Furthermore, this ratio of the boundary layer thickness over the half width of the duct for AR = 12 is almost identical to that for AR = 6. Additional heat transfer data were taken at every 1/16 L from the center to plot the entire surface profile of the Nusselt number from the center to the 1/16 L from the wall in Fig. 6. The surface plot shows a large increase in heat transfer in the rear of the cylinder. The effect of aspect ratio on the centerline Nusselt number is plotted in Fig. 7 for $Re = 6300$. Even at this low Reynolds number, the effect of the aspect ratio at the rear portion of the cylinder is distinct, though it is small. The effect is more pronounced for higher Reynolds number of 33,740 in Fig. 8. As the aspect ratio increases from 8.5 to 10.8, consistent decrease in *Nu* distribution at the rear of the cylinder is expected, but the present results show the effect of aspect ratio is not too significant for the two aspect ratios, 8.5 and 10.8.

Table 1 shows the centerline average Nusselt numbers; also, for $Re_D = 33,740$, the average over the complete cylinder is given. Two widely used correlations

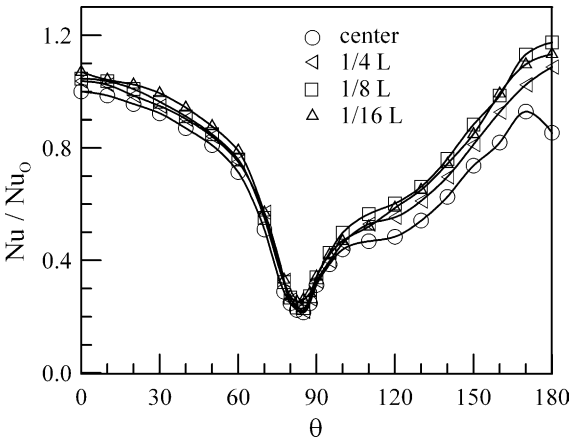

Fig. 4. Nusselt number profile for AR = 10.8, $Re = 33,740$.

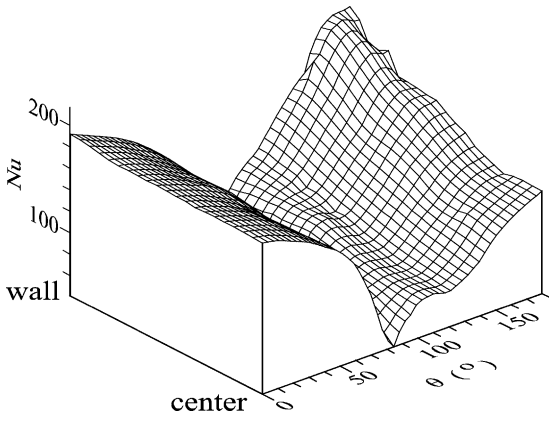

Fig. 6. Nusselt number profile for AR = 12, $Re = 33,740$.

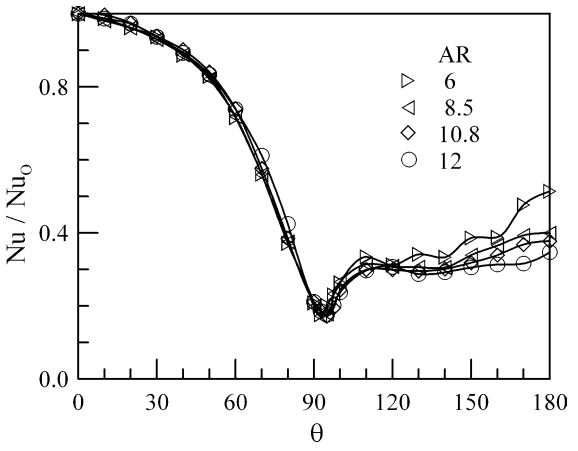

Fig. 7. Centerline Nusselt number profile for $Re = 6300$.

for $\overline{Nu}_D$ are those of Morgan [2] and Zukauskas [1]. Morgan corrected Hilpert's data [12] to account for air properties now in use, and recommends

$$\overline{Nu}_D = 0.148 Re_D^{0.633}, \quad 5 \times 10^3 < Re_D < 5 \times 10^4 \tag{2}$$

and claims an uncertainty of ±5%. Zukauskas recommends

$$\overline{Nu}_D = 0.23 Re_D^{0.6}, \quad 1 \times 10^3 < Re_D < 2 \times 10^5 \tag{3}$$

also with an uncertainty of about ±5%. For air in our Reynolds number range, Eq. (3) is almost identical to the correlation of Churchill and Bernstein [3],

$$\overline{Nu}_D = 0.3 + \frac{0.62 Re^{1/2} Pr^{1/3}}{[1 + (0.4/Pr)^{2/3}]^{1/4}} \left[1 + \left(\frac{Re}{282000}\right)^{5/8}\right]^{4/5} \tag{4}$$

Table 1 and Fig. 9 show that Eqs. (2) and (3) essentially bracket our results, which is reassuring. Since Eq. (2) gives the lowest values of $\overline{Nu}_D$ we can argue that augmentation due to free stream turbulence, tunnel blockage and aspect ratio are minimal. The blockage ratio for our tests was $D/H = 0.086$. Use of blockage and turbulence corrections recommended by Morgan [1] gives a correction factor of about 6%, which mostly explains the differences between our results and Morgan's correlation. Thus we choose to correlate the effect of aspect ratio we have obtained by addition of turbulence, blockage, and aspect ratio corrections to Morgan's correlation, Eq. (2),

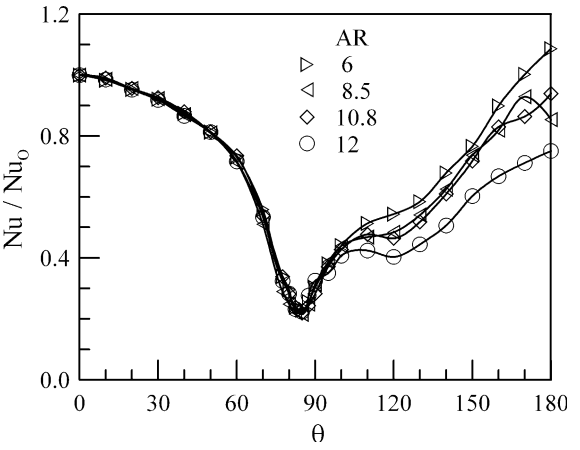

Fig. 8. Centerline Nusselt number profile for $Re = 33,740$.

$$\overline{Nu}_D = 0.148 Re_D^{0.633}[1 + 0.73(D/H)^{1.5} + 0.124(TU)^{0.64} + 1.764 \mathrm{AR}^{-1.5}], \quad 6 \leqslant \mathrm{AR} \leqslant 12 \tag{5}$$

which is shown in Fig. 10. The second and third terms in the bracket in Eq. (5) were derived from Morgan's graph on the combined effects of tunnel blockage and free stream turbulence. The fourth term is estimated to be $0.416\mathrm{AR}^{-0.5}$ for Nu_{avg}, the surface averaged Nusselt number; however, this result is based only on the data for $Re_D = 33,740$.

Table 1 also shows Nu_{avg}, Nusselt number averaged both circumferentially and spanwise at $Re_D = 33,740$. The value for AR = 12 is the integral under the area of the surface shown in Fig. 6, and is more accurate than for the smaller AR values for which fewer data points were available. For AR = 12 this Nu_{avg} is 11.5% higher than the centerline averaged value; for AR = 10.8, 8.5 and 6, the corresponding values are 7.1%, 6.5% and 2% respectively. As a result, Nu_{avg} shows less variation with AR than does $\overline{Nu}_D$ at the centerline, 4% versus 14%.

With the aspect ratio effect unambiguously established it is possible to evaluate evidence of this aspect ratio effect in some previous experimental studies. One study that shows a clear aspect ratio effect is that of

Table 1
Centerline circumferentially averaged Nusselt numbers $\overline{Nu}_D$ for various Reynolds numbers, and the circumferentially and spanwise averaged Nusselt number Nu_{avg} for $Re_D = 33,740$

Reynolds number	6300 $\overline{Nu}_D$	10,000 $\overline{Nu}_D$	19,480 $\overline{Nu}_D$	33,740 $\overline{Nu}_D$	33,740 Nu_{avg}	50,960 $\overline{Nu}_D$
AR = 6	43.6	56.8	89.9	130.6	133.2	166.7
8.5	41.8	56.2	85.6	124.8	132.9	157.5
10.8	42.3	56.0	85.7	125.7	134.7	155.9
12	41.8	54.9	80.0	114.9	128.2	150.0
Eq. (2)	37.6	50.4	76.8	108.8	–	141.2
Eq. (3)	44.0	58.0	86.6	120.4	–	154.2

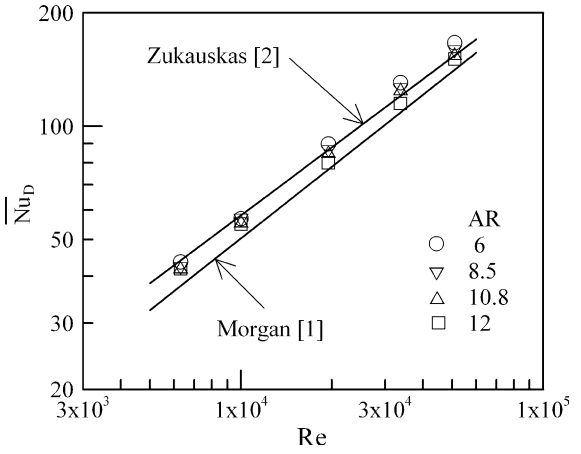

Fig. 9. Comparison with various correlations of the centerline circumferentially averaged Nusselt number.

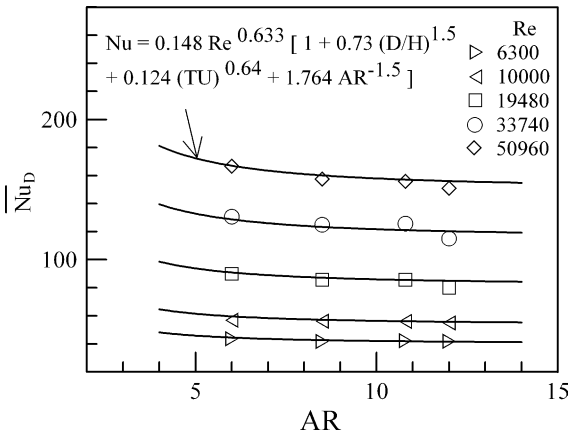

Fig. 10. Effect of aspect ratio on the circumferentially averaged Nusselt number.

Seban (AR = 3.9) [13]. At the lowest Reynolds number tested, $Re_D = 53,000$, $Nu_{180°}/Nu_{0°} \approx 1.3$, which is a reasonable extrapolation of the trend shown for $Re = 50,960$ in Table 1. However we must be careful to recognize that Seban's tube wall was heated at close to a uniform heat flux (UHF), rather than the uniform wall temperature (UWT) used in the present study. We will return to this point later. The often quoted results of Achenbach [7] were obtained for AR = 3.4, so a substantial aspect ratio effect can be expected. His local Nusselt number distributions were for $Re_D > 10^5$ and thus cannot be compared to our results. However, he presents average Nusselt numbers down to $Re_D = 3 \times 10^4$, and his Fig. 12 shows values of $\overline{Nu}$ about 40% higher than those of Hilpert [12] at $Re_D = 30,000$. His blockage ratio and turbulence level were 16.4% and 0.45% respectively, which could explain around 12% of this increase using the corrections given by Morgan [2]. Thus there is clear evidence of a substantial aspect ratio effect in Achenbach's data.

Murray and Fitzpatrick [14] report results for an aspect ratio of 12 and 12% tunnel blockage at UWT: Fig. 11 shows their heat transfer results on the rear of the cylinder for $Re = 33,200$ agree well with the present results for AR = 12 and $Re = 33,740$ which supports the reliability of our rear cylinder data. However, near the forward stagnation line, our Nusselt number decreases more rapidly than those in Ref. [14], and indeed with theory. At $\theta = 30°$, $Nu/Nu_{0°}$ is 0.92, as compared

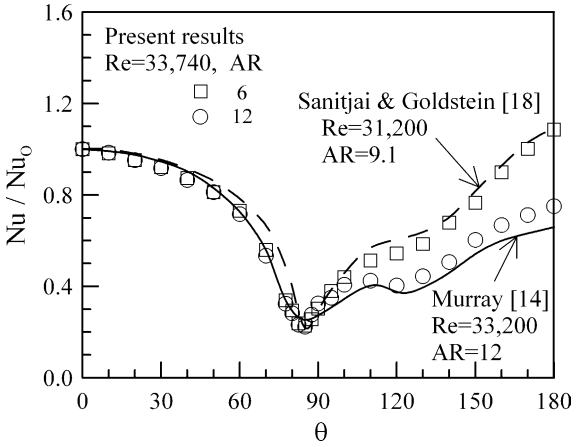

Fig. 11. Nusselt number profiles for different aspect ratios.

with 0.94 from Frossling's theoretical distribution [15]. We have been unable to determine the reason for this discrepancy. Scholten and Murray [16] actually show an increase in Nusselt number up to $\theta = 10°$ even after correcting for the insulating effect of the hot film sensor substrate. Murray and Fitzpatrick [14] also show the Nusselt number distribution obtained by Schmidt and Wenner [17] at $Re_D = 33,920$ for which $Nu_{180°}/Nu_{0°} \approx 1.0$, indicating an aspect ratio or blockage effect. Achenbach shows that $\overline{Nu}_D$ obtained by these authors was also substantially higher than Hilpert's value [12], confirming the above observation.

The distinctive feature of the aspect ratio effect in our Reynolds number range of 6×10^3–5×10^4 are significantly increased heat transfer rates on the rear of the cylinder. Sanitjai and Goldstein [18] have recently reported results for local mass transfer using the naphthalene sublimation technique. This technique gives an analog to a UWT heat transfer experiment, though the Schmidt number of 2.35 is somewhat higher than the 0.7 Prandtl number for air. Their test cylinder had aspect ratio of 9 and a tunnel blockage ratio of 0.11. At low turbulence levels for $3 \times 10^4 < Re_D < 6 \times 10^4$, the mass transfer coefficients on the rear of the cylinder were 13–37% higher than the stagnation line values. Even after accounting for a 7% blockage and turbulence level correction, these values are considerably larger than obtained in the present study. Their measured profile for $Re_D = 31,200$ is compared with present results in Fig. 11, and it is close to our results for AR = 6. The actual spanwise location where the data were measured is not given in the paper, but in a private communication we were informed that data was obtained in location where no spanwise variation was in evidence [19]. We are unable to explain why their transfer rates are so high on the cylinder rear, but no explanation of this anomalous results is given in Ref. [18] either. The test section with the naphthalene spanned only 55% of the tunnel height and was stationed at the bottom wall, and not at the center of the tunnel. The measurements may have been made off-centered, thus resulting in high transfer rates on the rear. At $Re_D = 31,200$, their $\overline{Nu}_D$ is 138.6, and this is about 34% higher than the value from Morgan's correlation.

Baughn et al. [20] obtained data for AR = 20% and 8.3% tunnel blockage with a UHF cylinder. At $Re_D = 20,000$ they obtained $Nu_{180°}/Nu_{0°} = 1$. Since the combined blockage and turbulence effects are 7–8%, $Nu_{180°}$ is unexpectedly high. The cause of this *effect* is possibly related to the wall thermal boundary condition: local heat transfer coefficients are higher for UHF versus UWT for boundary layer flows, and can be quite different for separated flows [21]. Papell [22] heated a cylinder at both UWT and UHF and found UWT heat transfer coefficients at 80° were up to 66% lower than for UHF. Unfortunately, he did not obtain data for $\theta > 100°$. Baughn and Saniei [23] show Nu profiles for both UHF and UWT up to 150° with higher heat transfer rates for UWT at 150°. On the other hand, the results of van Meel [9] obtained with AR = 14, 7.2% blockage, and a wall boundary condition closer to UHF than UWT do not show this *effect*.

West and Apelt [24] performed hydrodynamic studies with AR from 4 to 10, and blockage ratio from 2% to 16%. The drag coefficient was found to vary smoothly with aspect ratio, and the change was more rapid at small aspect ratio. They found that reduction in aspect ratio had similar effects on the drag coefficient as the increase in blockage ratio. Their study and the present study show that the effect of aspect ratio needs to be studied with the other parameters kept invariant.

3. Conclusions

1. The effect of aspect ratio on heat transfer to a cylinder in cross flow has been unambiguously established for the parameter range tested.
2. As the aspect ratio decreases below 12, heat transfer rates at the center plane on the rear of cylinder increase markedly, resulting in an increase in the circumferentially averaged Nusselt number.
3. At an aspect ratio of 12, the local Nusselt number on the rear of the cylinder increase as the wall is approached; at an aspect ratio of 6 the local Nusselt numbers are almost constant along the cylinder (at the high value noted above).
4. A number of anomalies in data in the literature can be explained by proper recognition of the aspect ratio effect.
5. Further studies of the combined tunnel blockage and aspect ratio effects might be useful.

Acknowledgements

Ranjit Darke and Tiffany Groode performed a preliminary investigation. Dale Cooper and Miguel Lozano supplied technical support for construction of the apparatus. Their help is gratefully acknowledged.

References

[1] A.A. Zukauskas, Heat transfer from tubes in cross flow, Adv. Heat Transfer 8 (1972) 116–133.
[2] V.T. Morgan, The overall convective heat transfer from smooth circular cylinders, Adv. Heat Transfer 11 (1975) 199–264.
[3] S.W. Churchill, M. Bernstein, A correlating equation for forced convection from gases and liquids to a circular cylinder in crossflow, J. Heat Transfer 99 (May) (1977) 300–306.

[4] A. Quarmby, A.A.M. Al-Fakhri, Effect of finite length on forced convection heat transfer from cylinders, Int. J. Heat Mass Transfer 23 (1980) 463–469.
[5] J.C.R. Hunt, C.J. Abell, J.A. Peterka, H. Woo, Kinematical studies of the flow around free or surface-mounted obstacles, J. Fluid Mech. 86 (1978) 179–200.
[6] R.J. Goldstein, J. Karni, The effect of a wall boundary layer on local mass transfer from a cylinder in crossflow, J. Heat Transfer 106 (May) (1984) 260–267.
[7] E. Achenbach, Total and local heat transfer from a smooth circular cylinder in cross-flow at high Reynolds number, Int. J. Heat Mass Transfer 18 (1975) 1387–1396.
[8] W.M. Kays, M.E. Crawford, Convective Heat and Mass Transfer, third ed., McGraw-Hill, 1996.
[9] D.A. van Meel, A method for the determination of local convective heat transfer from a cylinder placed normal to an air stream, Int. J. Heat Mass Transfer 5 (1962) 715–722.
[10] J. Kestin, P. Maeder, Influence of turbulence on transfer of heat from cylinders, NACA TN 4018, 1956.
[11] J.W. Scholten, D.B. Murray, Heat transfer in the separation and wake regions of a gas-particle cross flow, in: Proceedings of 10th International Heat Transfer Conference, Brighton, vol. 1, England, 1994, pp. 375–380.
[12] R. Hilpert, Warmeabgabe von geheizten Drahten und Rohren im LuftstromForschungsarbeiten aufdem Gebiete des Ingenienrwesens 4 (1933) 215–224.
[13] R.A. Seban, The influence of free stream turbulence on the local heat transfer from cylinders, J. Heat Transfer 82 (1960) 101–107.
[14] D.B. Murray, J.A. Fitzpatrick, Local heat transfer coefficients for tube array using a micro-foil heat flow sensor, in: Proceedings of 2nd UK National Conference on Heat Transfer, vol. 2, 1988, pp. 1635–1649.
[15] H. Schlichting, Boundary Layer Theory, seventh ed., McGraw-Hill, 1979, pp. 304–305.
[16] J.W. Scholten, D.B. Murray, Unsteady heat transfer and velocity of a cylinder in cross flow—I. Low freestream turbulence, Int. J. Heat Mass Transfer 41 (10) (1998) 1139–1148.
[17] E. Schmidt, K. Wenner, Heat transfer over the circumference of a heated cylinder in a transverse flow, NACA TM 1050, 1943.
[18] S. Sanitjai, R.J. Goldstein, Effect of free stream turbulence on local mass transfer from a circular cylinder, Int. J. Heat Mass Transfer 44 (2001) 2863–2875.
[19] R. Goldstein, Private Communication, February 2003.
[20] J.W. Baughn, M.J. Elderkin, A.A. Mckillop, Heat transfer from a single cylinder, cylinders in tandem, and cylinders in the entrance region of a tube bank with a uniform heat flux, J. Heat Transfer 108 (1986) 386–391.
[21] B.H. Chang, A.F. Mills, Effect of wall thermal boundary conditions on heat transfer to separated flow, J. Enhanced Heat Transfer 5 (1998) 1–12.
[22] S.S. Papell, Influence of thermal boundary conditions on heat transfer from a cylinder in cross flow, NASA Technical Paper 1894 (1981).
[23] J.W. Baughn, N. Saniei, The effect of the thermal boundary condition on heat transfer from a cylinder in crossflow, J. Heat Transfer 113 (1991) 1020–1023.
[24] G.S. West, C.J. Apelt, The effects of tunnel blockage and aspect ratio on the mean flow pst a circular cylinder with Reynolds numbers between 10^4 and 10^5, J. Fluid Mech. 114 (1982) 361–377.